ACS APPLIED MATERIALS & INTERFACES

Letter

www.acsami.org

Three-Dimensional Layer-by-Layer Anode Structure Based on Co_3O_4 Nanoplates Strongly Tied by Capillary-like Multiwall Carbon Nanotubes for Use in High-Performance Lithium-Ion Batteries

Tae Il Lee,[†,‡] Jong-Pil Jegal,[†,§] Ji-Hyeon Park,[§] Won Jin Choi,[⊥] Jeong-O Lee,[⊥] Kwang-Bum Kim,*[,§] and Jae-Min Myoung*[,§]

[‡]College of BioNano Technology, Gachon University, Gyeonggi 461-701, Korea

[§]Department of Materials Science and Engineering Yonsei University , 134 Shinchon-dong, Seodaemoon-gu, Seoul, Korea

[⊥]Advanced Materials Division, Korea Research Institute of Chemical Technology (KRICT), Daejeon 305-343, Korea

Supporting Information

ABSTRACT: A layer-by-layer (LBL) structure composed of Co_3O_4 nanoplates and capillary-like three-dimensional (3D) multiwall carbon nanotube (MWCNT) nets was developed as an anode with simultaneous high-rate and long-term cycling performance in a lithium-ion battery. As the current density was increased to 50 A g^{-1}, the LBL structure exhibited excellent long-term cycling and rate performance. Thus, the Co_3O_4 nanoplates were in good electrical contact with the capillary-like 3D MWCNT nets under mechanically severe strain during long-term, high-rate cyclic operation.

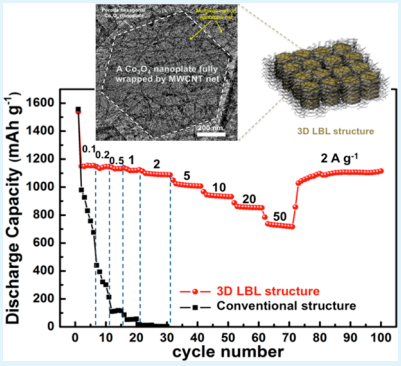

KEYWORDS: *layer by layer, Li ion battery, carbon nanotube, cobalt oxide, nanoplate*

The charge and discharge rates in a given electrochemical cell depend on how fast the redox reaction progresses. Unless the lithium ions between the electrolyte and the redox sites and the electrons between the redox sites and the collecting electrode are rapidly transported, high-rate performance cannot be obtained.[1−3] Meanwhile, the long-term cycling stability relies on the mechanical stress−strain, which are generated by the volume expansion and contraction of the anode material and are relieved during the redox cycle, where the anode material electrochemically reacts with lithium ions. Maintaining an electrical connection between the anode-active material and the conducting material is thus the key to ensuring long-term cycling performance.[4−6]

The development of an anode with both high-rate and long-term cycling characteristics is highly desirable for lithium-ion battery technology. However, no effective methods for imparting both of these characteristics to an anode material currently exist.[7,8]

To design an anode configuration with these two key properties, we here introduce a strategy in which various nanomaterial layers and multistacking layers are used to construct a layer-by-layer (LBL) structure. In this structure, capillary-like three-dimensional (3D) multiwall carbon nanotube (MWCNT) nets provide electrically perfect addressing on and mechanically strong wrapping of each anode-active nanomaterial against its large volume expansion during redox cycle. Especially, the producing cost of MWCNT is cheaper than that of the other conductor materials such as reduced graphene oxide or single wall CNT so that it can easily be commercialized. We experimentally demonstrate the capability of this strategy using cobalt oxide (Co_3O_4) nanoplates as anode-active nanomaterials.[9−13]

Figure 1a shows the process for constructing the 3D LBL structure consisting of multistacked layers of porous Co_3O_4 nanoplates that are perfectly addressed and strongly wrapped by capillary-like MWCNT nets. The layers of MWCNT nets and α-$Co(OH)_2$ nanoplates were both prepared on a deionized water surface using our previously reported method[14] (Videos S1 and S2 in the Supporting Information). Three layers were sequentially transferred to copper foil, as shown in Figure 1b, c. After α-$Co(OH)_2$ was transformed into Co_3O_4 and residual water molecules were eliminated through thermal annealing at 300 °C for 2 h in air, the anode was completed, as shown in Figure 1d. High-resolution transmission electron microscopy (TEM) images of α-$Co(OH)_2$ nanoplates and Co_3O_4 nanoplates are shown in Figure S1 in the Supporting Information. During the thermal annealing, the single-crystalline α-$Co(OH)_2$ nanoplates were converted into porous and polycrystalline

Received: November 27, 2014
Accepted: February 9, 2015
Published: February 9, 2015

DOI: 10.1021/am5083599
ACS Appl. Mater. Interfaces 2015, 7, 3861−3865

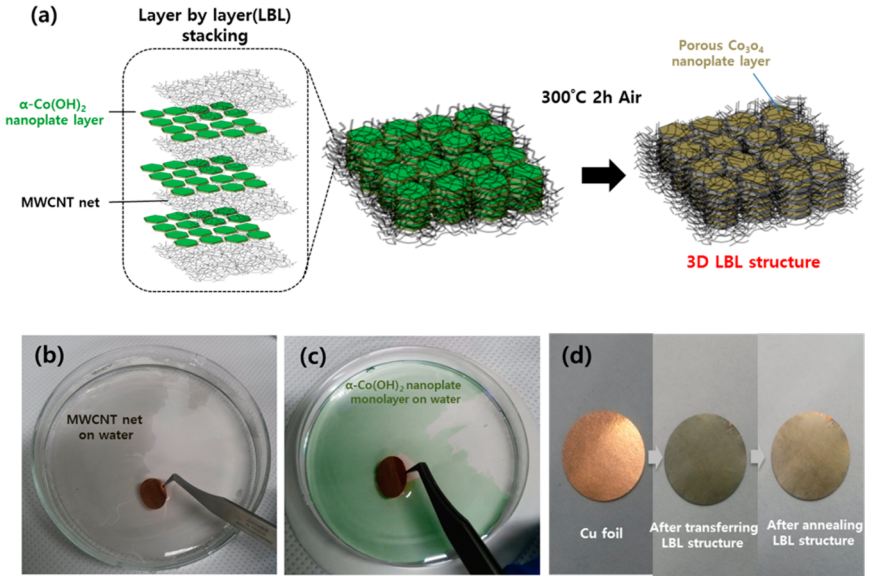

Figure 1. (a) Schematic of the sequential process used to construct the 3D LBL structures consisting of Co_3O_4 nanoplates and capillary-like 3D MWCNT nets. (b) Scooping a 2D MWCNT net floating on water onto a Cu foil. (c) Transferring a layer α-$Co(OH)_2$ nanoplate floating on water onto Cu foil. (d) Change in color of the Cu foil after the LBL structure is transferred and annealed.

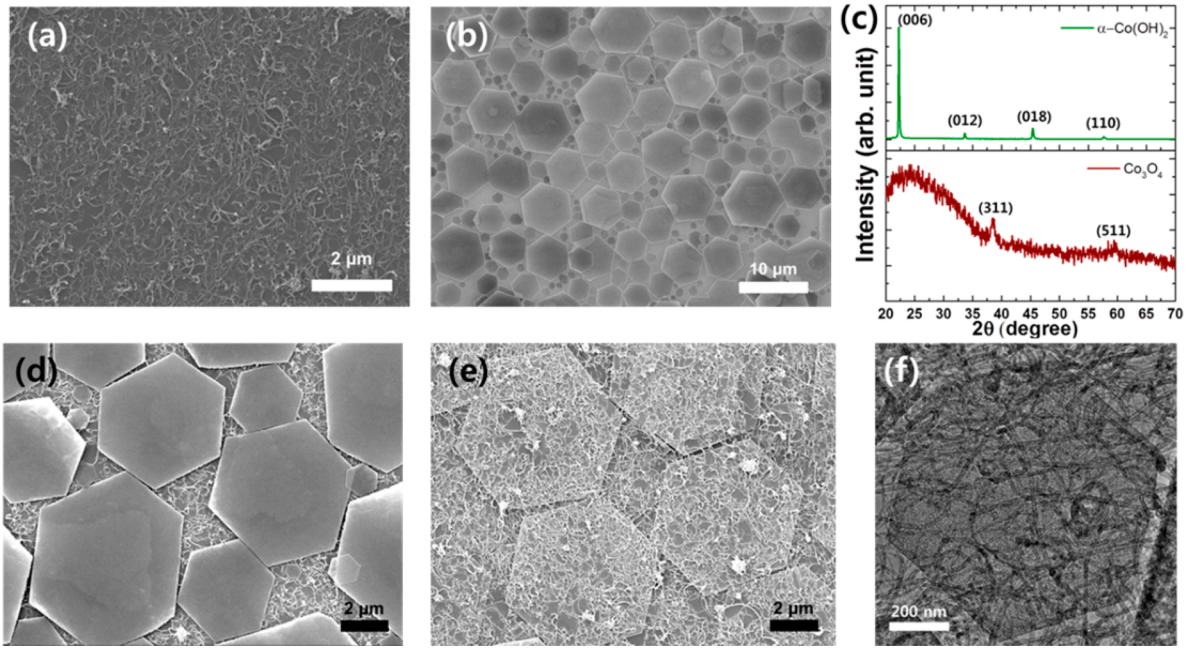

Figure 2. (a) Top-view SEM image of a 2D MWCNT net. (b) Top-view SEM image of a layer of α-$Co(OH)_2$. (c) XRD spectra before and after thermal annealing of a layer of α-$Co(OH)_2$ on a glass substrate. (d) Top-view SEM image of a layer of α-$Co(OH)_2$ on a 2D MWCNT net during stacking of the LBL structure. (e) Top-view SEM image of a 2D MWCNT net on a layer of α-$Co(OH)_2$ during stacking of the LBL structure. (f) TEM image of a Co_3O_4 nanoplate wrapped by 2D MWCNT nets.

Co_3O_4 nanoplates. The change in chemical composition of the α-$Co(OH)_2$ nanoplates by thermal annealing was investigated using scanning electron microscopy (SEM) energy-dispersive X-ray spectroscopy (EDS), as shown in Figure S2 in the Supporting Information. Initially, the EDS signals from chloride atoms, which originate from the precursor (cobalt chloride hexahydrate), were detected from the α-$Co(OH)_2$ nanoplates; however, no EDS signals of chloride atoms were observed from the Co_3O_4 nanoplates.

As shown in Figure 2a, the pore size of a two-dimensional (2D) MWCNT film was approximately several hundred nanometers and the film was shaped like a continuous fishing-net-like layer. This nanoporous net structure provides an electrically conductive and mechanically strong frame for use as a high-performance anode. Hexagonal α-$Co(OH)_2$ nanoplates wrapped by the MWCNT net were placed on a substrate with *c*-axis orientation in a brucite structure to form the film shown in Figure 2b. The presence of the nanoplates before and after thermal annealing was confirmed through X-ray diffraction (XRD) analysis, as shown in Figure 2c.

During construction of a unit of the LBL structure, the α-$Co(OH)_2$ nanoplates were placed on a MWCNT net, as shown

DOI: 10.1021/am5083599
ACS Appl. Mater. Interfaces 2015, 7, 3861−3865

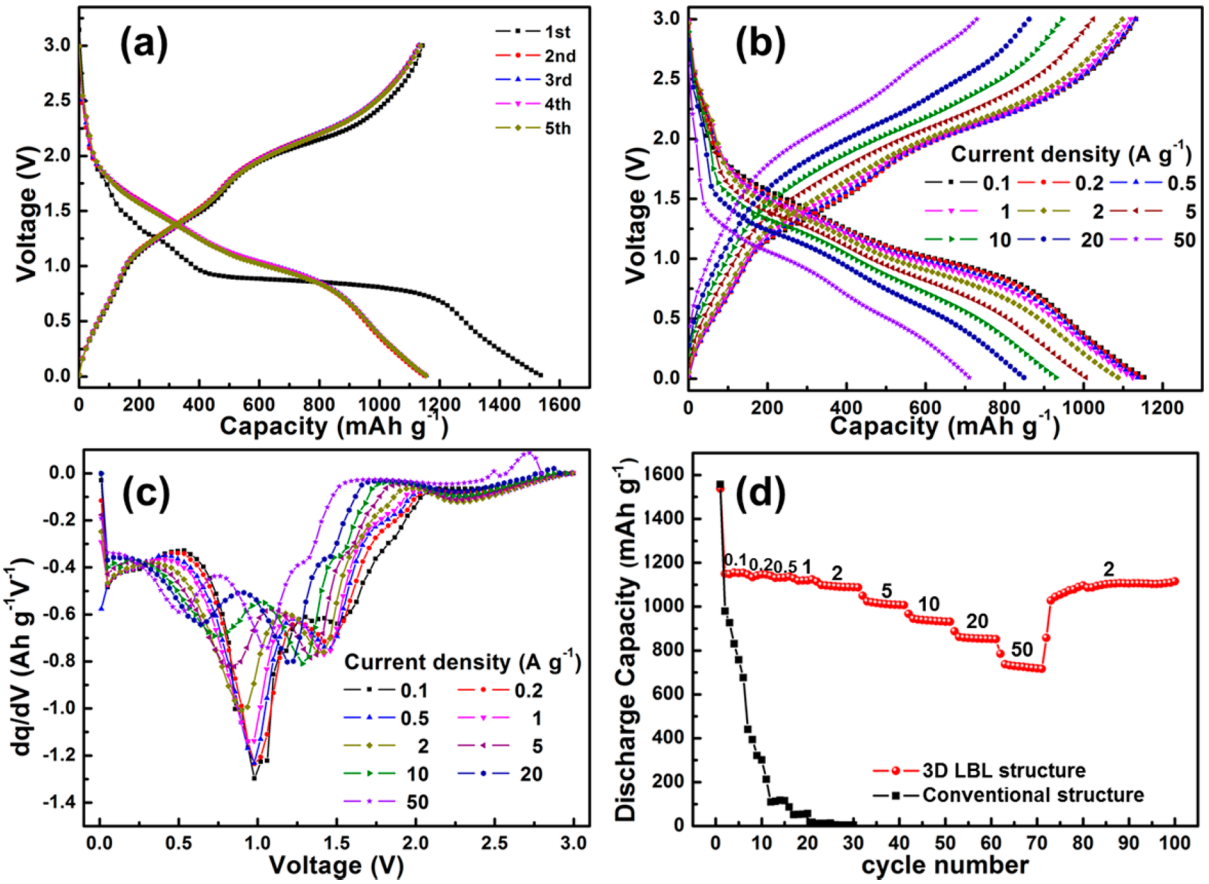

Figure 3. (a) Discharge profiles of the triple LBL structures at a current density of 0.1 A g^{-1} for the first 5 cycles. (b) Discharge profiles of the triple LBL structures at current densities from 0.1 to 50 A g^{-1}. (c) Differential discharge capacity of the triple LBL structure at current densities from 0.1 to 50 A g^{-1}. (d) Capacity retention at different current densities of the triple LBL structure and control electrode fabricated using the conventional slurry method from Co_3O_4 nanoparticles, carbon black, and a binder.

in Figure 2d, such that the bottom sides of all of the nanoplates were electrically addressable by the MWCNT net. Next, another MWCNT net was placed on the nanoplates, as shown in Figure 2e. As a result, the nanoplates are perfectly enveloped by MWCNT nets and the top and bottom MWCNT nets tighten with each other through the gaps between the α-$Co(OH)_2$ nanoplates. By repeated stacking in this manner, a 3D LBL structure was produced, where the MWCNT nets enveloped the surface of each α-$Co(OH)_2$ nanoplate, as shown in Figure 2f. To evaluate the performance of the 3D LBL structure as a Li-ion battery anode, we constructed three sets of MWCNT net/α-$Co(OH)_2$ nanoplates on Cu foil.

Figure 3a shows the discharge profiles of the LBL structure at a current density of 0.1 A g^{-1} for the first 5 cycles. The first discharge curve exhibits two different behaviors: a sloping discharge at the beginning and a potential plateau in the middle. This surface effect, which has been reported for numerous nanostructured materials, results in a sloping potential profile that can be applied to the LBL structure because the Co_3O_4 nanoplates in the LBL structure are approximately 10 nm thick.[15,16] The potential plateau is accompanied by the full conversion reaction of Co_3O_4 and the formation of a solid-electrolyte interface (SEI).[17] Reductive dissociation of the salts or additives is used to construct the ion-conductive coating layer (i.e., the SEI) on the surface of the anode. This reaction continuously and irreversibly consumes Li ions as the fresh surface is exposed. The discharge capacity of the LBL structure at the first cycle is approximately 1550 mAh g^{-1} on the basis of the weight of the total electrode composed of the Co_3O_4 nanoplates and the MWCNT nets; this capacity is much greater than the theoretical capacity of Co_3O_4. This greater-than-theoretical capacity may be caused by the formation of the SEI and the subsequently storage of Li^+ ions in the interface. Guo et al. reported that extra Li^+ ions can be stored on the ionic-conducting side of the interface by an interfacial Li storage mechanism and this mechanism is enhanced in nanosized materials because of their extremely large interface areas.[14] The subsequent 4 cycles show sloping discharge profiles with almost identical discharge capacities of approximately 1155 mAh g^{-1}, irrespective of the cycle number. Again, this discharge capacity was higher than the theoretical capacity, possibly because of an interfacial Li storage mechanism in the nanosized electrode materials.[18,19] The stable cycle properties of the LBL structure demonstrate perfect electrical addressing to the Co_3O_4 nanoplates, despite repeated volume expansion and extraction during the conversion reaction. This perfect electrical addressing was possible because the Co_3O_4 nanoplates were strongly wrapped by the capillary-like MWCNT nets. CNTs have been reported to act as elastic bodies to external mechanical forces,[20] which, would allow them to provide structural integrity to the LBL structure during the repeated volume changes of the Co_3O_4 nanoplates. The sloping discharge profile is due to amorphization of the Co_3O_4 during the conversion reaction in the first cycle.[21,22] In contrast

DOI: 10.1021/am5083599
ACS Appl. Mater. Interfaces 2015, 7, 3861−3865

to the LBL structure, the control electrode, which was fabricated using the conventional slurry method from Co_3O_4 nanoparticles, carbon black, and a binder, exhibited continuous capacity fade during cycling (see Figure S3 in the Supporting Information). This capacity fade indicates that the electrical contact between the Co_3O_4 nanoparticles and the carbon black gradually decreased because of the large volume change of the Co_3O_4 nanoparticles during repeated cycling.

At increasing current densities, this LBL structure exhibited excellent rate performance up to a current density of 50 Ag^{1-}, as shown in Figure 3b. Its discharge capacity at current densities up to 1 A g^{-1} changed only slightly, and it retained capacities greater than 1000 mAh g^{-1} at current densities up to 5 A g^{-1}. Moreover, it sustained a discharge capacity of approximately 710 mAh g^{-1} at a current density as high as 50 A g^{-1}. To the best of our knowledge, this material exhibits better rate performance than any Co_3O_4-based anode material reported in the literature. This excellent rate performance is attributed to the full addressing of the Co_3O_4 nanoplates with the capillary-like highly conductive MWCNT nets and the short travel length of electrons and Li^+ ions through the thin *c*-axis of the Co_3O_4 nanoplates. In addition, Li^+ ions in the bulk electrolyte can be immediately supplied to the electroactive sites (i.e., the surface of the Co_3O_4 nanoplates), as the MWCNT nets act as electrolyte reservoirs because of their 3D porous nature.

To better explain the excellent rate performance of the LBL structure, we plotted the differential capacities in Figure 3c. Two broad peaks are present in the 1.5−1.0 V and 1.0−0.5 V ranges, regardless of the current density. The first peak is ascribed to the intercalation of Li^+ ions into the Co_3O_4 to form an intermediate $Li_xCo_3O_4$ phase. The second peak is ascribed to the full reduction of the intermediate phase to Co metal.[21] Notably, an intermediate $Li_xCo_3O_4$ phase is always formed upon reduction of Co_3O_4 to metallic Co.[23,24] Also notable is the observation that the peaks associated with intercalation shift in the negative direction with little change in intensity, whereas the intensity of the conversion-reaction peaks gradually decreases and the peaks shift in the negative direction with increasing current density. These behaviors indicate that the capacity loss at high rates is mainly due to the slow kinetics of the conversion reaction, which accompanies a phase transformation. Meanwhile, little capacity is lost by the formation of the intermediate $Li_xCo_3O_4$ phase via the intercalation of Li^+ ions, even at very high current densities. Because the intermediate phase is more stable under high current densities, it can sustain high capacities at high rates.[20] The peak in the differential capacity is clearly separated between the intercalation and conversion reactions because of the full electronic and ionic addressing of the Co_3O_4 nanoplates with the capillary-like highly conductive 3D porous MWCNT nets.

Figure 3d shows the long-term cycling performance of the LBL structure at various current densities. The control electrode exhibited a drastic decrease in capacity. Even at low current densities, it could not sustain its capacity when the current density exceeded 2 A g^{-1}. In contrast, the LBL structure could sustain high discharge capacities at current densities as high as 50 A g^{-1}. Its capacity was fully recovered when the current density was returned to 2 A g^{-1}. This behavior demonstrates that the Co_3O_4 nanoplates were in good contact with the conductive MWCNT nets during repeated cycling because they were sandwiched between the MWCNT nets. To support the structural sustainability of the LBL structure, we observed its microstructure after 100 cycles. The hexagonal shapes of the Co_3O_4 nanoplates were preserved, and each nanoplate was stably addressed within the MWCNTs (see Figure S4a, b in the Supporting Information).

In conclusion, we introduced a design strategy for a Li-ion battery anode that provides both high-rate performance and long-term cycling performance. This strategy involves an LBL structure formed by sequential multistacking of 2D MWCNT nets and anode-active nanomaterial layers. These structures are rapidly produced by dropping an alcohol containing each nanomaterial onto pure water. After the stacking is complete, the LBL structure has a frame consisting of capillary-like 3D MWCNT nets that provide perfect electrical addressing and mechanically strong wrapping of the anode-active nanomaterials. The LBL structures were fabricated using Co_3O_4 nanoplates as an anode-active material, and their performance was demonstrated. As the current density was increased to 50 A g^{-1}, the LBL structure exhibited excellent long-term cycling and rate performance. Little change was observed in the discharge capacity up to a current density of 1 A g^{-1}, and a capacity greater than 1000 mAh g^{-1} was retained at current densities as high as 5 A g^{-1}. Moreover, at a current density as high as 50 A g^{-1}, the discharge capacity was sustained at approximately 710 mAh g^{-1}. The capacity was then fully recovered when the current density was returned to 2 A g^{-1} after 75 cycles. This performance demonstrates that the Co_3O_4 nanoplates were in good electrical contact with the 3D MWCNT nets despite the mechanically severe strain during long-term, high-rate cycling operation because they were tightly bound to the electrically conductive 3D MWCNT nets. Although Co_3O_4 nanoplates were used as an example of a volume-expanding anode material in Li-ion batteries to verify the viability of our strategy, we believe that electrically conductive and mechanically strong frames based on capillary-like 3D MWCNT nets can prevent other anode nanomaterials, such as Si, Fe_2O_3, MnO, and SnO, from deteriorating because of huge volume changes during redox processes.

■ ASSOCIATED CONTENT

Supporting Information

Videos S1 and S2, formation of layers of MWCNTs and α-$Co(OH)_2$ nanoplates; experimental details; Figure S1, SEM images and EDS spectrum of the α-$Co(OH)_2$ and Co_3O_4 nanoplates; Figure S2, high-resolution TEM images of the α-$Co(OH)_2$ and Co_3O_4 nanoplates; Figure S3, continuous capacity fading upon cycling of the control electrode fabricated by the conventional slurry method; Figure S4, top-view SEM image of the layer-by-layer structure and a high-resolution transmission electron microscopy image of multiwall carbon nanotubes on the surface of cobalt oxide nanoplates after 100 cycles; the certificate of BET analysis for Co_3O_4 nanoplates. This material is available free of charge via the Internet at http://pubs.acs.org.

■ AUTHOR INFORMATION

Corresponding Authors

*E-mail: kbkim@yonsei.ac.kr.
*E-mail: jmmyoung@yonsei.ac.kr.

Author Contributions

†T.I.L. and J.-P.J. equally contributed to this work

Notes

The authors declare no competing financial interest.

DOI: 10.1021/am5083599
ACS Appl. Mater. Interfaces 2015, 7, 3861−3865

■ ACKNOWLEDGMENTS

This research was supported by WCU program through the National Research Foundation of Korea funded by the Ministry of Education, Science and Technology [R32-20031] and by the LG Display academic industrial cooperation program. This work was also supported by the National Research Foundation (NRF) of Korea Grant funded by the Korean Government (MSIP) (NRF-2011-0030542).

■ REFERENCES

(1) Tarascon, J. M.; Armand, M. Review Article Issues and Challenges Facing Rechargeable Lithium Batteries. *Nature* **2001**, *414*, 359−367.

(2) Lee, Y. J.; Yi, H. J.; Kim, W. J.; Kang, K. S.; Yoon, D. S.; Strano, M. S.; Ceder, G.; Belcher, A. M. Fabricating Genetically Engineered High-power Lithium-ion Batteries Using Multiple Virus Genes. *Science* **2009**, *324*, 1051−1055.

(3) Wang, H. L.; Cui, L. F.; Yang, Y.; Casalongue, H. S.; Robinson, J. T.; Liang, Y. Y.; Cui, Y.; Dai, H. J. Mn_3O_4-Graphene Hybrid as a High-Capacity Anode Material for Lithium Ion Batteries. *J. Am. Chem. Soc.* **2010**, *132*, 13978−13980.

(4) Yu, Y.; Gu, L.; Zhu, C. B.; P. Aken, A. V.; Maier, J. Tin Nanoparticles Encapsulated in Porous Multichannel Carbon Microtubes: Preparation by Single-Nozzle Electrospinning and Application as Anode Material for High-Performance Li-Based Batteries. *J. Am. Chem. Soc.* **2009**, *131*, 15984−15985.

(5) Ban, C. M.; Wu, Z. C.; Gillaspie, D. T.; Chen, L.; Yan, Y. F.; Blackburn, J. L.; Dillon, A. C. Nanostructured Fe_3O_4/SWNT Electrode: Binder-Free and High-Rate Li-Ion Anode. *Adv. Mater.* **2010**, *22*, E145−149.

(6) Lee, K. T.; Jung, Y. S.; Oh, S. M. Synthesis of Tin-Encapsulated Spherical Hollow Carbon for Anode Material in Lithium Secondary Batteries. *J. Am. Chem. Soc.* **2003**, *125*, 5652−5653.

(7) Kim, H. G.; Seo, D. H.; Kim, S. W.; Kim, J. S.; Kang, K. S. Highly Reversible Co_3O_4/graphene Hybrid Anode for Lithium Rechargeable Batteries. *Carbon* **2011**, *49*, 326−332.

(8) Wu, Z. S.; Ren, W. C.; Wen, L.; Gao, L. B.; Zhao, J. P.; Chen, Z. P.; Zhou, G. M.; Li, F.; Cheng, H. M. Graphene Anchored with Co3O4 Nanoparticles as Anode of Lithium Ion Batteries with Enhanced Reversible Capacity and Cyclic Performance. *ACS Nano* **2010**, *4*, 3187−3194.

(9) Wang, G. X.; Chen, Y.; Konstantinov, K.; Lindsay, M.; Liu, H. K.; Dou, S. X. Investigation of Cobalt Oxides as Anode Materials for Li-ion Batteries. *J. Power Sources* **2002**, *1*, 142−147.

(10) Wang, G. X.; Chen, Y.; Konstantinov, K.; Yao, J.; Ahn, J.-h.; Liu, H. K.; Dou, S. X. Nanosize Cobalt Oxides as Anode Materials for Lithium-ion Batteries. *J. Alloys Compd.* **2002**, *1*−*2*, L5−L10.

(11) Yang, S.; Cui, G.; Pang, S.; Cao, Q.; Kolb; Feng, U. X.; Maier, J.; Mllen, K. Fabrication of Cobalt and Cobalt Oxide/Graphene Composites: Towards High-Performance Anode Materials for Lithium Ion Batteries. *ChemSusChem* **2010**, *3*, 236−239.

(12) Li, W.-Y.; Xu, L.-N.; Chen, J. Co_3O_4 Nanomaterials in Lithium-Ion Batteries and Gas Sensors. *Adv. Funct. Mater.* **2005**, *5*, 851−857.

(13) Li, Y.; Tan, B.; Wu, Y. Mesoporous Co3O4 Nanowire Arrays for Lithium Ion Batteries with High Capacity and Rate Capability. *Nano Lett.* **2008**, *8*, 265−270.

(14) Lee, T. I.; Jeagal, J. P.; Choi, J. H.; Choi, W. J.; Lee, M. J.; Oh, J. Y.; Kim, K. B.; Baik, H. K.; Xia, Y. N.; Myoung, J. M. Binder-Free and Full Electrical-Addressing Free-Standing Nanosheets with Carbon Nanotube Fabrics for Electrochemical Applications. *Adv. Mater.* **2011**, *23*, 4711−4715.

(15) Wang, J.; Polleux, J.; Lim, J.; Dunn, B. Pseudocapacitive Contributions to Electrochemical Energy Storage in TiO_2 (Anatase) Nanoparticles. *J. Phys. Chem. C* **2007**, *111*, 14925−14931.

(16) Larcher, D.; Masquelier, C.; Bonnin, D.; Chabre, Y.; Masson, V.; Leriche, J.-B.; Tarascon, J.-M. Effect of Particle Size on Lithium Intercalation into α-Fe_2O_3. *J. Electrochem. Soc.* **2003**, *150*, A133−139.

(17) Taberna, P. L.; Mitra, S.; Poizot, P.; Simon, P.; Tarascon, J.-M. High Rate Capabilities Fe_3O_4-based Cu Nano-architectured Electrodes for Lithium-ion Battery Applications. *Nat. Mater.* **2006**, *5*, 567.

(18) Guo, Y. G.; Hu, J. S.; Wan, L. J. Nanostructured Materials for Electrochemical Energy Conversion and Storage Devices. *Adv. Mater.* **2008**, *20*, 2878.

(19) Du, N.; Zhang, H.; Chen, B. D.; Wu, J. B.; Ma, X. Y.; Liu, Z. H.; Zhang, Y. Q.; Yang, D. R.; Huang, X. H.; Tu, J. P. Porous Co_3O_4 Nanotubes Derived from $Co_4(CO)_{12}$ Clusters on Carbon Nanotube Templates: A Highly Efficient Material for Li-battery Applications. *Adv. Mater.* **2007**, *19*, 4505.

(20) Natsuki, T.; Tantrakarn, K.; Endo, M. Prediction of Elastic Properties for Single-Walled Carbon Nanotubes. *Carbon* **2004**, *42*, 39−45.

(21) Poizot, P.; Laruelle, S.; Grugeon, S.; Dupont, L.; Tarascon, J.-M. Nano-sized Transition-metal Oxides as Negative-electrode Materials for Lithium-ion Batteries. *Nature* **2000**, *407*, 496−499.

(22) Tarascon, J.-M.; Grugeon, S.; Morcrette, M.; Laruelle, S.; Rozier, P.; Poizot, P. New Concepts for the Search of Better Electrode Materials for Rechargeable Lithium Batteries. *C. R. Chim.* **2005**, *8*, 9−15.

(23) Larcher, D.; Sudant, G.; Leriche, J.-B.; Chabre, Y.; Tarascon, J.-M. The Electrochemical Reduction of Co_3O_4 in a Lithium Cell. *J. Electrochem. Soc.* **2002**, *149*, A234−241.

(24) Thackeray, M. M.; Baker, S. D.; Adendorff, K. T.; Goodenough, J. B. Lithium Insertion into Co_3O_4: A Preliminary Investigation. *Solid State Ionics* **1985**, *17*, 175−181.

DOI: 10.1021/am5083599
ACS Appl. Mater. Interfaces 2015, 7, 3861−3865